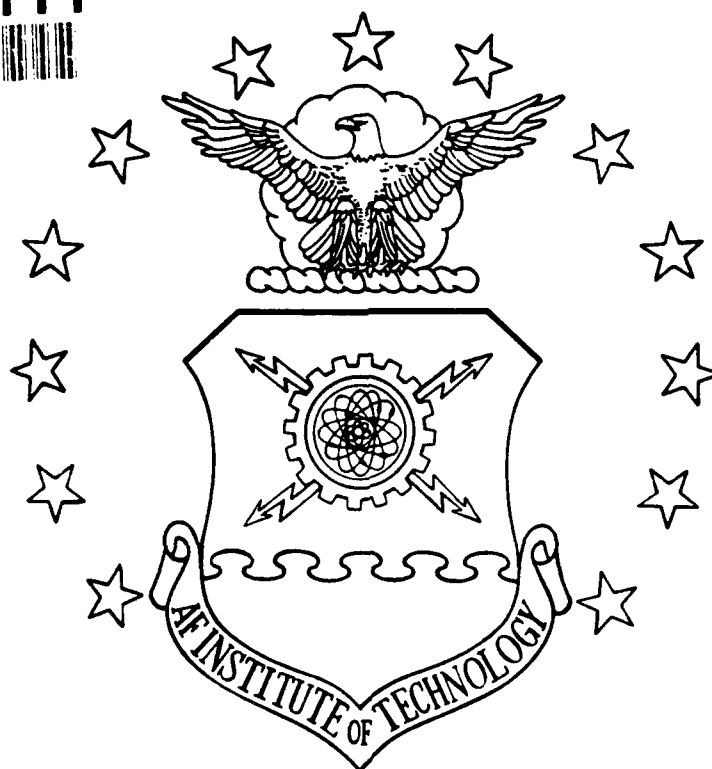


AD-A248 111



DTIC  
ELECTE  
APR 01 1992  
S B D



MODEL OF A NUCLEAR THERMAL  
TEST PIPE USING ATHENA

THESIS

Mark J. Dibben, Captain, USAF

AFIT/GNE/ENP/92M-2

DISTRIBUTION STATEMENT A  
Approved for public release;  
Distribution Unlimited

92-08151



DEPARTMENT OF THE AIR FC  
AIR UNIVERSITY

**AIR FORCE INSTITUTE OF TECHNOLOGY**

92 3 31 098 Wright-Patterson Air Force Base, Ohio

0000 0000 0000

AFIT/GNE/ENP/92M-2

MODEL OF A NUCLEAR THERMAL  
TEST PIPE USING ATHENA

THESIS

Mark J. Dibben, Captain, USAF

AFIT/GNE/ENP/92M-2

REPORT DOCUMENTATION PAGE			Form Approved OMB No. 0704-0188	
Public reporting burden for this collection of information is estimated to average 1 hour per response, including the time for reviewing instructions, searching existing data sources, gathering and maintaining the data needed, and completing and reviewing the collection of information. Send comments regarding this burden estimate or any other aspect of this collection of information, including suggestions for reducing this burden, to Washington Headquarters Services, Directorate for Information Operations and Reports, 1215 Jefferson Davis Highway, Suite 1204, Arlington, VA 22202-4302, and to the Office of Management and Budget, Paperwork Reduction Project (0704-0188), Washington, DC 20503.				
1. AGENCY USE ONLY (Leave blank)		2. REPORT DATE March 1992		3. REPORT TYPE AND DATES COVERED Master's Thesis
4. TITLE AND SUBTITLE  MODEL OF A NUCLEAR THERMAL TEST PIPE USING ATHENA			5. FUNDING NUMBERS	
6. AUTHOR(S)  Mark J. Dibben, Captain, USAF				
7. PERFORMING ORGANIZATION NAME(S) AND ADDRESS(ES)  Air Force Institute of Technology, WPAFB OH 45433-6583			8. PERFORMING ORGANIZATION REPORT NUMBER  AFIT/GNE/ENP/92M	
9. SPONSORING / MONITORING AGENCY NAME(S) AND ADDRESS(ES)  MARLAND L. STANLEY EG&G IDAHO, INC P.O. BOX 1625 Idaho Falls ID 83415			10. SPONSORING / MONITORING AGENCY REPORT NUMBER	
11. SUPPLEMENTARY NOTES				
12a. DISTRIBUTION / AVAILABILITY STATEMENT  Approved for public release; distribution unlimited			12b. DISTRIBUTION CODE	
13. ABSTRACT (Maximum 200 words)  Nuclear thermal propulsion offers significant improvements in rocket engine specific impulse over rockets employing chemical propulsion. The computer code ATHENA (Advanced Thermal Hydraulic Energy Network Analyzer) was used in a parametric analysis of a fuelpipe. The fuelpipe is an annular particle bed fuel element of the reactor with radially inward flow of hydrogen through it. The outlet temperature of the hydrogen is parametrically related to key effects, including the effect of reactor power at two different pressure drops, the effect of the power coupling factor of the Annular Core Research Reactor, and the effect of hydrogen flow. Results show that the outlet temperature is linearly related to the reactor power and nonlinearly to the change in pressure drop. The linear relationship at higher temperatures is probably not valid due to dissociation of hydrogen. Once thermal properties of hydrogen become available, the ATHENA model for this study could easily be modified to test this conjecture.				
14. SUBJECT TERMS  Nuclear Propulsion, Nuclear Reactors, ATHENA, Propulsion Systems, Computerized Simulation			15. NUMBER OF PAGES 72	
			16. PRICE CODE	
17. SECURITY CLASSIFICATION OF REPORT Unclassified	18. SECURITY CLASSIFICATION OF THIS PAGE Unclassified	19. SECURITY CLASSIFICATION OF ABSTRACT Unclassified	20. LIMITATION OF ABSTRACT UL	

AFIT/GNE/ENP/92M-2

MODEL OF A NUCLEAR THERMAL  
TEST PIPE USING ATHENA

THESIS

Presented to the Faculty of the School of Engineering  
of the Air Force Institute of Technology  
Air University  
In Partial Fulfillment of the  
Requirements for the Degree of  
Master of Science in Nuclear Engineering

Mark J. Dibben, B.S.

Captain, USAF

March 1992

Approved for public release; distribution unlimited

## Preface

The purpose of this study was to develop a simulation of a fuel pipe using the computer code ATHENA. It originally started out as a short research project but the installation of the program took more than half of the quarter.

Thanks are in order to my faculty advisor, Col Tuttle, for allowing me to continue to work on this project even after he left this organization. Dr. Elrod was also helpful in obtaining information for me concerning properties of hydrogen.

I would also like to thank several people at INEL for the assistance they have given me on this project. Dick Wagner successfully installed ATHENA after we had failed and helped me with parts of the programming. Tony Zuppero answered questions for me concerning the project and found other people at INEL to help me.

Final thanks go to my family. Jason, Luis, and Amanda have been an inspiration and deserve lots of my time now that this is finished.

Accession For	
NTIS	<input checked="" type="checkbox"/>
DO	<input type="checkbox"/>
US	<input type="checkbox"/>
Accession Number	
By	
Director	
Availability Status	
Accession Number	
Dist	

## Table of Contents

Preface .....	ii
List of Figures .....	iv
List of Tables .....	v
Abstract .....	vi
I Introduction .....	1
1.1 Background .....	1
1.2 Problem and Scope .....	3
1.3 Particle Bed Reactor .....	3
1.4 Nuclear Thermal Rocket .....	4
1.5 Literature Review .....	5
II The ATHENA Code .....	9
2.1 RELAP5 Code Description .....	9
2.2 Expanded Capabilities of ATHENA .....	11
III Modeling of the Fuelpipe .....	12
3.1 Availability of data .....	12
3.2 Layout of the Volumes .....	12
3.2.1 Modeling of the Hydrodynamic Volumes .....	14
3.2.2 Modeling of the Heat Structures .....	16
3.2.3 Boundary Conditions .....	17
IV Results and Discussion .....	19
4.1 Base Case .....	19
4.2 Constant Pressure Drop .....	22
4.3 Higher Pressure Drop .....	24
4.4 Coupling Factor .....	26
4.5 Mass Flow Rate .....	27
V Conclusions and Recommendations .....	31
Appendix A: Graphics Strip Program .....	32
Appendix B: Graphics Modification Program .....	34
Appendix C: Sample Input File .....	37
Bibliography .....	63
Vita .....	65

### List of Figures

Diagram of Fuelpin .....	4
Dissociation of Hydrogen .....	8
Layout of Fuelpipe Volumes .....	13
Outlet Temperature for Base Case .....	20
Temperature Profile of Base Case .....	21
Temperature Comparison at Low Flow .....	23
Temperature Comparison at High Flow .....	24
Comparison of Outlet Temperatures at Both Flow Rates .....	25
Pressure Drop vs Flow Rate .....	27
Mass Cross Flow at Axial Junctions .....	29
Outlet Temperature vs Flow Rate .....	30

List of Tables

Fuelpipe Parameters .....	14
Power Distribution .....	16
Initial Conditions for Base Case .....	20
Observed Outlet Temperature for Change in Coupling Factor .....	26



### Abstract

Nuclear thermal propulsion offers significant improvements in rocket engine specific impulse over rockets employing chemical propulsion. The computer code ATHENA (Advanced Thermal Hydraulic Energy Network Analyzer) was used in a parametric analysis of a fuelpipe. The fuelpipe is an annular particle bed fuel element of the reactor with radially inward flow of hydrogen through it. The outlet temperature of the hydrogen is parametrically related to key effects, including the effect of reactor power at two different pressure drops, the effect of the power coupling factor of the Annular Core Research Reactor, and the effect of hydrogen flow. Results show that the outlet temperature is linearly related to the reactor power and nonlinearly to the change in pressure drop. The linear relationship at higher temperatures is probably not valid due to dissociation of hydrogen. Once thermal properties of hydrogen become available, the ATHENA model for this study could easily be modified to test this conjecture.

## MODEL OF A NUCLEAR THERMAL TEST PIPE USING ATHENA

### I Introduction

#### 1.1 Background

In 1989 the President Bush proposed the Space Exploration Initiative (SEI). This proposal called for astronauts to return to the Moon and to go to Mars early in the 21st century. To develop this proposal, Vice President Quayle and National Aeronautics and Space Administration administrator Richard H. Truly formed the Synthesis Group whose goal was to study ideas and suggestions for America's space program (Synthesis Group, 1991:86). Their recommendations call for the development of both the nuclear thermal rocket and space nuclear power technologies. The nuclear thermal rocket can be used to reduce the travel time to Mars from the estimated 450-500 days for chemical rockets to only 120-180 days. This reduced travel time will help to minimize the astronauts exposure to solar and galactic radiation (Asker, 1991b:39 2 Dec). Boeing Space & Defense Group has also analyzed different propulsion systems for spacecraft to Mars and has determined that nuclear thermal is better than

chemical, solar electric, or nuclear electric propulsion (Asker, 1991a:24 18 Mar 1991).

The manned mission to Mars is not the only use for the nuclear thermal rocket. Ramsthaler and Sulmeisters (1988:21) have determined that among nuclear thermal, chemical, and nuclear electric, the direct-thrust nuclear stage is the most cost effective propulsion system for performing the LEO (Low Earth Orbit) to GEO (Geosynchronous Earth Orbit) orbit transfer mission. They have concluded that the direct thrust nuclear rocket engine should be the priority Air Force development system for orbital maneuvering and transfer mission.

Particle Bed Reactors (PBR) are the power source in nuclear thermal rockets. Lazareth and others (1987:223) outline four objectives PBR's meet that allow them to potentially power space-based weapon systems as well. They can be integrated into Strategic Defense Initiative weapons, they can deliver full power in just a few seconds, they can operate at hundreds to thousands of megawatts of power, and finally they can operate for hundreds to thousands of seconds. These characteristics are ideal for space-based weapons.

### 1.2 Problem and Scope

Idaho National Engineering Laboratory has been contracted by the Air Force Astronautical Laboratory as the overall program manager for the development of the nuclear engine (Ramsthaller and Sulmeisters, 1988:19). During this program, INEL has asked AFIT to make a computer simulation of one part of this nuclear thermal rocket, a fuelpin. The purpose of this thesis is to model this fuelpin and to determine the thermal hydraulic flow characteristics within it. The computer code ATHENA (Advanced Thermal Hydraulic Energy Network Analyzer) will be used to make this simulation.

### 1.3 Particle Bed Reactor

The fuelpin that will be modeled is one element of a particle bed reactor. It consists of small fuel particles confined in an annulus between two concentric frits (Figure 1). The fuel particles are made of a uranium carbide kernel surrounded by a layer of graphite and coated with zirconium carbide to prevent chemical reactions with hydrogen. Hydrogen flows radially inward through the fuel bed and is then exhausted axially through the channel formed by the inner frit. The porosity of the outer, or cold frit, can be varied axially to maintain a uniform temperature along the inner or hot frit. By changing the porosity of the frit,

the hydrogen mass flow rate is changed. This is necessary because of variations in the shape of the power curve (Benenati and others, 1987:139).

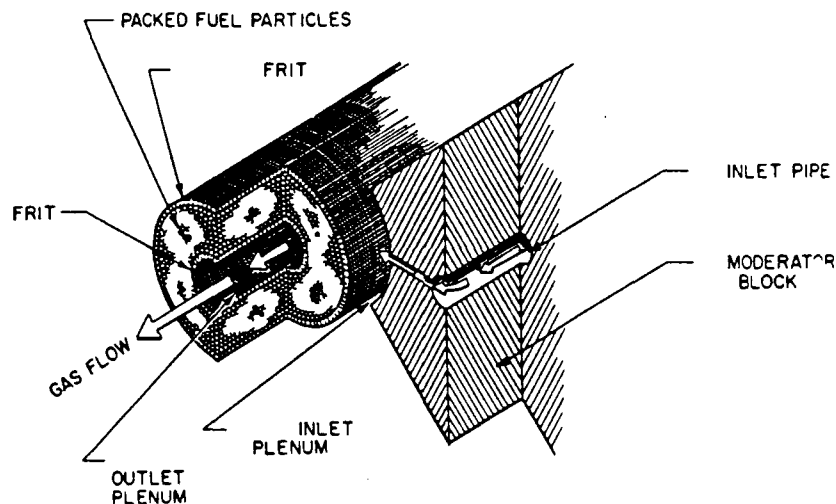


Figure 1. Diagram of Fuelpin (Lazareth, 1987:225)

#### 1.4 Nuclear Thermal Rocket

One design for a nuclear thermal rocket uses 19 of these fuel elements arranged in a moderator. After the propellant flows through the fuel elements, it is then ejected through the rocket nozzle. An indicator of rocket engines is the specific impulse. It is proportional to the square root of the gas temperature at the nozzle inlet and inversely proportional to the square root of the molecular weight of the exhaust gas. To increase the specific impulse, the

propellant temperature must be increased and the molecular weight of the propellant decreased. For most systems, this implies a hydrogen propellant operating at as high of temperature as possible (Araj and others, 1988:85). In a particle bed reactor, the highest temperatures are seen in the innermost part of the fuel bed, the hot frit and the exhaust channel. Therefore, the temperature is limited by the materials these sections are made of. If hafnium is substituted for zirconium in these high temperature areas, the maximum temperature can be raised to 3600 K instead of 3200 K for zirconium materials (Leyse and others, 1990:2).

The specific impulse for chemical engines is about 500 seconds while some low pressure nuclear thermal rockets have analytically reached over 1250 seconds. The dissociation of hydrogen is attributed with some of this increase in specific impulse, but because of uncertainties in the kinetics of hydrogen dissociation/recombination, its contribution may be questionable (Leyse and others, 1990a:2). However, even without the benefits of dissociation, the specific impulse offered by nuclear thermal rockets is much greater than any achieved by chemical rockets.

### 1.5 Literature Review

RELAP5 (Reactor Excursion and Leak Analysis Program) is the code from which ATHENA is derived. A review of the lit-

erature found no other RELAP5 models similar to a particle bed reactor. The primary use of RELAP5 is in modeling light water reactors for loss of coolant accidents and other transient failures. When the ATHENA code became available three other models of a similar nature to this project were found. Two of these modeled the SP-100 (Fletcher, 1986:Chapter 10 and Roth, 1987:Chapter 46). One other model simulated a simplified version of a fuel pipe (Roth, unpublished).

The review also found a lack of property data for the materials used in a particle bed reactor. Specifically, thermal properties for ZrC and UC<sub>2</sub> were not found above 2800-3000K while this project required data to at least 3200 K and possibly to 3600 K. Heat capacities were available for ZrC to 3000 K and for UC to 2800 (Storms, 1967:29, 201). A secondary source listed thermal conductivity data for ZrC to 3000 K and for UC<sub>2</sub> to 3200 K (Smalec, 1990:99, 103), while a primary source listed data to only 2100 K for UC and 2700 for ZrC (Touloukian and others, 1970:109, 609).

The same data was required for pyrolytic graphite. The value of these properties varied up to two orders of magnitude depending on the density and direction of propagation of heat (Touloukian and others, 1970:30-31, 41). More specific information regarding these materials is needed to ensure proper treatment.

Hydrogen property data is also lacking. It is known

that hydrogen dissociates as the temperature is increased and the dissociation becomes even greater as the pressure is decreased as shown in Figure 2. At 20 atmospheres dissociation begins at 2800 K and is ten percent dissociated by 3500 K. This range also happens to be the operating range for a nuclear thermal rocket. This dissociation will change the thermal properties of hydrogen allowing it to carry away more heat from the fuel. This additional heat capacity of the hydrogen lowers the temperature in the core, thus permitting the reactor to operate at a higher power. Dissociation will also increase the pressure of the hydrogen by increasing the number of molecules which in turn will increase the specific impulse of a rocket. Although all of this is known, the property data is not available to allow adequate modeling. INEL has initiated an experiment for providing this needed data (Leyse, 1990b:1), but it is not yet available. As a result, modeled outlet temperatures from the reactor will exceed actual temperatures in most cases.



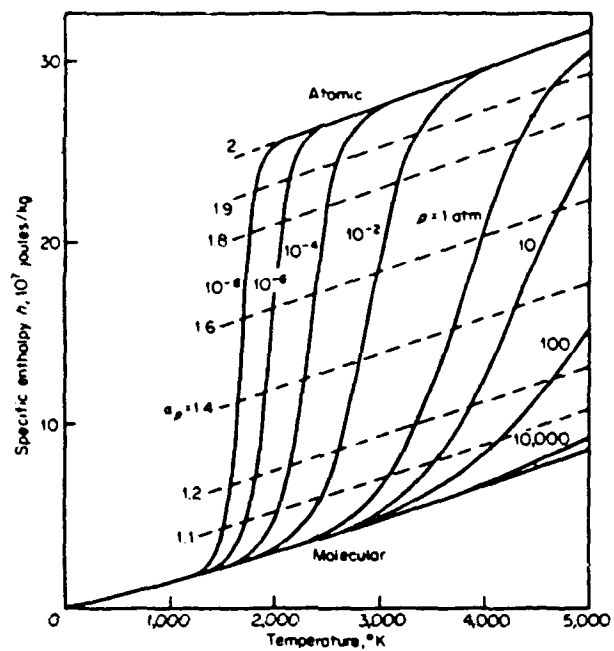


Figure 2. Dissociation of Hydrogen (Jahn, 1968:97)

## II The ATHENA Code

The RELAP5 (Reactor Excursion and Leak Analysis Program) computer code was developed at the Idaho National Engineering Laboratory (INEL) for the U. S. Nuclear Regulatory Commission (NRC). The ATHENA code is an expanded version of the RELAP5 code, which has become an industry standard for light water reactors. It can be used to model the thermal hydraulics of complete energy generation and/or conversion systems at normal operating conditions and during off-normal transients (Roth, undated:1).

### 2.1 RELAP5 Code Description

The RELAP5 code is based on a nonhomogeneous and non-equilibrium model for the two-phase system that is solved by a fast, partially implicit numerical scheme to permit economical calculation of system transients. The code includes many generic models that are used as the basic structure to make more complex systems. These models include pumps, valves, pipes, heat structures, reactor point kinetics, electric heaters, jet pumps, turbines, separators, accumulators, and control system components. Because of limited knowledge of systems and because of finite computer resources, many approximations are used in the code. For example, two phase flow is not fully understood. Also, items such as spatial nodalization are required to be of a

finite size. It is not possible to calculate the pressure at every single point along a pipe. The approximations used in this code are necessary to model real systems and allow them to be solved in a reasonable amount of time (Carlson and others, 1990:iv, 1-5).

Generally, modeling a system with RELAP5 is divided into two sections - hydrodynamics and heat flow. The hydrodynamic model is based on the use of fluid control volumes and junctions that represent the actual flow of fluid in the system. Control volumes are connected together with junctions at the inlet and outlet to model the flow path of the fluid. Fluid scalar properties such as pressure, energy and density are averaged over the entire cell volume and located at the center of the control volume. Vector properties such as fluid velocities are located at the junctions.

Heat flow models are used to represent heat structures such as pipe walls, heater elements, nuclear fuel pins and heat exchanger surfaces. Heat structures are thermally connected to the hydrodynamic control volumes. For example, if the wall of a pipe could exchange heat with the fluid flowing within it, the pipe wall would be connected to the control volume of fluid.

Neither RELAP5 nor ATHENA currently have graphics capability. However, during a simulation, information can be saved at certain time intervals to a plot file. A small

program is then used to create a strip file, shown in Appendix A, to extract information used in making graphs. This strip file was then modified with another program, shown in Appendix B, to create files that can be read by programs such as TK or Freelance.

## 2.2 Expanded Capabilities of ATHENA

The major difference between RELAP5 and ATHENA is ATHENA's ability to model working fluids other than water. These include hydrogen, helium, lithium, sodium and potassium. Two eutectic liquid fluids are available: LiPb (17 atom percent lead) and NaK (22.2 weight percent sodium). ATHENA can also be modified to specify any acceleration due to gravity. Normally, it is set to the earth's surface value but it can also be set to zero for space applications. It is because of the features of RELAP5 and the upgrades to ATHENA that this code was selected for this project.

### III Modeling of the Fuelpipe

#### 3.1 Availability of data

The primary source of information used for making this simulation was obtained from L. M. Smalec's technical data record (Smalec, 1990). In some cases, because of a lack of information, certain assumptions had to be made. These and all other aspects of the simulation will be documented as they are presented. This simulation models an experimental setup but is not compared to any data because it was not available at the time of this work.

#### 3.2 Layout of the Volumes

For this simulation, it was chosen to divide the fuelpipe into five regions axially and seven regions radially, one section in the inlet channel, five sections in the fuel bed and one section in the exhaust channel as shown in Figure 3. This was done to adequately represent the change in temperature and pressure through the fuelbed. Volumes 60 and 62 represent boundary conditions. The hydrogen enters from volume 60 and flows into the inlet channel, volumes 1-5. It then flows radially through the fuel bed, volumes 6-30. The heated hydrogen is exhausted through volumes 31-35 to the outlet boundary condition, volume 62. Junctions connect each of the volumes both radially and axially

to include cross flow within the fuelbed. A total of 37 hydrodynamic volumes and 60 junctions are required to be modeled.

The measurements and characteristics assumed for this fuelpipe are shown in Table 1. These physical characteristics of the fuelpipe must be translated into a format readable by ATHENA. This is done by creating an input deck. This input deck contains the geometry of the hydrodynamic volumes, areas of junctions connecting the volumes, initial input status, heat structure data including thermal properties of all materials used in the system and finally, the power table. A typical input deck is shown in Appendix C.

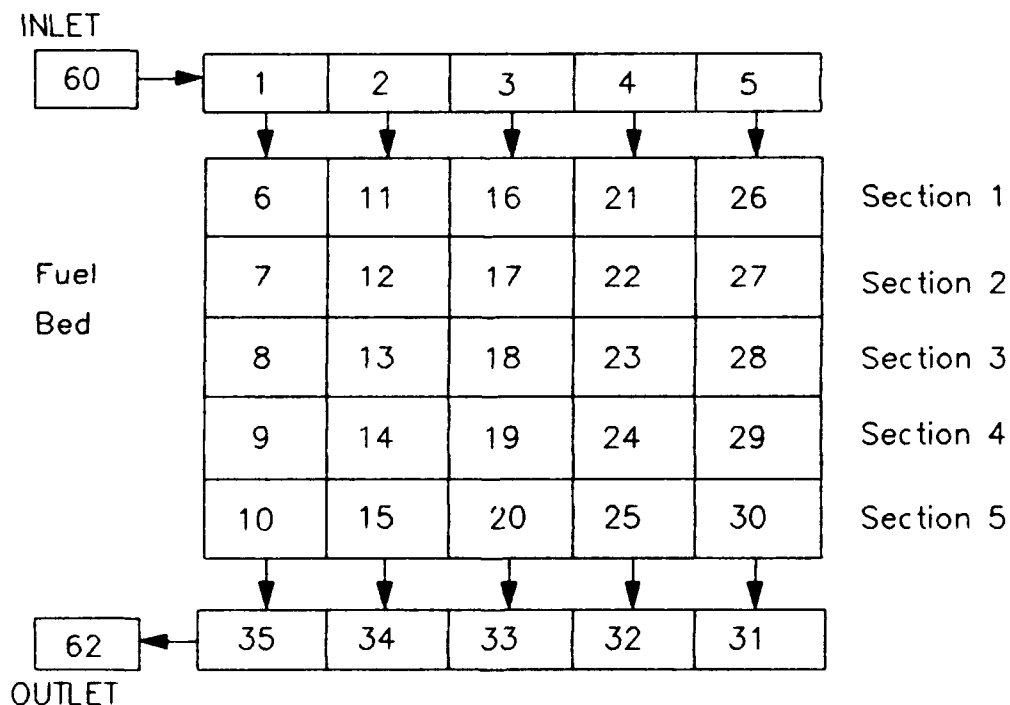


Figure 3. Layout of Fuel Volumes

Table 1.

## Fuelpipe Parameters

Length of active bed	25.4 cm
Outlet plenum id	2.85 cm
hot frit thickness	0.15 cm
cold frit id	5.50 cm
cold frit thickness	0.51 cm
inlet plenum od	8.92 cm
coupling factor to ACRR	33.0 W/MW/cm <sup>3</sup>
fuel bed volume	428.5 cm <sup>3</sup>
fuel pellet	
Uranium carbide od	0.240 mm
LTI od	0.304 mm
pyrolytic graphite od	0.404 mm
zirconium carbide od	0.500 mm
void fraction	0.36

3.2.1 Modeling of the Hydrodynamic Volumes The major consideration in modeling the hydrodynamic volumes is the geometry. Based on the dimensions previously shown in Table 1, the volumes were divided equally in the axial direction. They were also divided radially so as to have the same radial length. The calculation of the volume of the hydrodynamic volume is based on the space occupied by the hydrogen. This excludes any space occupied by the fuel particles. Therefore, the actual volume of hydrogen is found by multiplying by the void fraction of 0.36. The flow area is also affected by the fuel particles. The corrected volume divided by the radial length of each cell gives the flow area so that each hydrodynamic volume is consistent in

its dimensions.

Friction factors were calculated for the flow through the packed bed. This is based on the equation

$$K = \frac{\Delta P 2g_c \rho A^2}{\dot{m}}$$

K = flow energy loss coefficient

$g_c$  = gravitational constant

$\rho$  = density of hydrogen

A = flow area

$\dot{m}$  = mass flow rate of hydrogen

It was found that this factor was nearly constant for varying flow rates.

One point of departure from the technical data record is the hydraulic diameter. It is listed as 500  $\mu\text{m}$ , the diameter of the fuel particles. Another reference (Bennett, 1982:212) equates the hydraulic diameter for flow through a packed bed to the following equation

$$r_H = \frac{1}{6} \frac{\epsilon}{(1 - \epsilon)} D$$

$r_H$  = hydraulic radius

$\epsilon$  = void fraction

D = diameter of particle



The hydraulic diameter is then twice the hydraulic radius. This yields a hydraulic diameter of 93.8  $\mu\text{m}$ . This value has been used in all subsequent calculations.

3.2.2 Modeling of the Heat Structures More work was required to determine the needed parameters for the heat structures. The primary heat structure is the fuel. It is thermally linked to the hydrodynamic volumes (hydrogen). The assumed power distribution is shown in Table 2. The numbers represent relative power levels. Axially, the power is lower on the ends and increases towards the middle. Because each radial section has decreasing volume as it approaches the inside of the annulus, the power also decreases radially inward.

Table 2

Power Distribution

		Axial				
Radial		1	2	3	4	5
	1	1.4685	1.6355	1.6895	1.6482	1.5083
	2	1.0963	1.2210	1.2613	1.2304	1.1260
	3	0.8506	0.9473	0.9787	0.9547	0.8737
	4	0.6715	0.7478	0.7725	0.7536	0.6896
	5	0.5311	0.5914	0.6110	0.5960	0.5454

ATHENA requires heat capacity and thermal conductivity data for all heat structure materials for the entire range of encountered temperatures. As mentioned previously, much

of this data is not available. The lack of accurate data is a serious deficiency in this simulation. Where possible, existing data has been extrapolated to cover the range of interest. Because of the large variation in the thermal properties for graphite, a constant value for heat capacity and thermal conductivity were used.

The fuel pipe was powered by being brought into contact with the Annular Core Research Reactor (ACRR). The power scaling factor between the ACRR and fuelpipe is determined by

$$\text{Power scaling factor} = \text{coupling factor} \times \text{bed volume}$$

The coupling factor is assumed to be  $33 \text{ W/MW/cm}^3$ , while the bed volume is fixed at  $428.5 \text{ cm}^3$ . By multiplying this factor by the ACRR power, the total power being developed in the bed is calculated.

**3.2.3 Boundary Conditions** The area of interest for this project was the fuelpipe itself. By concentrating on this the rest of the nuclear thermal rocket was ignored. What happened to the hydrogen gas before it reached the inlet to the fuelpipe was ignored. Therefore, initial conditions were set at the inlet of the pipe to specify the temperature

and pressure of the hydrogen. Specifying the pressure at the outlet boundary condition designates the pressure drop across the entire pipe. Because of forward flow, the suggested outlet temperature was inconsequential since the temperature of the previous volume is the outlet temperature. Given the inlet and outlet pressures, pressure drops across all boundaries are also specified. This also determines the flow rate of hydrogen throughout the system.

#### IV Results and Discussion

The specifications for the baseline case that was used as a reference for this study are outlined in Table 3. The parameters that were individually studied are ACRR power at two different pressure drops, the coupling factor and the flow rate of hydrogen.

##### 4.1 Base Case

Using the conditions of Table 3, the temperature of the hydrogen gas was calculated as it exits the fuelpipe. This is presented in Figure 4 as a function of time. It is clear that the maximum temperature of 804 K has been reached within five seconds. This same equilibrium time was observed in all of the other simulations. It also compares very well to results obtained by Lazareth and others (1987:225). Using a different program, they obtained maximum reactor coolant temperature in 4.4 seconds. This short equilibrium time allows the computer simulations to be completed within twenty four hours on the Sun workstations making a parametric study possible. Unless otherwise noted, all outlet temperatures will be based on this five second period.

Table 3

Initial Conditions for Base Case

Inlet H <sub>2</sub> temperature	300 K
Inlet H <sub>2</sub> pressure	2.068 MPa
Outlet H <sub>2</sub> pressure	2.02 MPa
ACRR Power	16 MW
Coupling Factor	33 W/MW/cm <sup>3</sup>

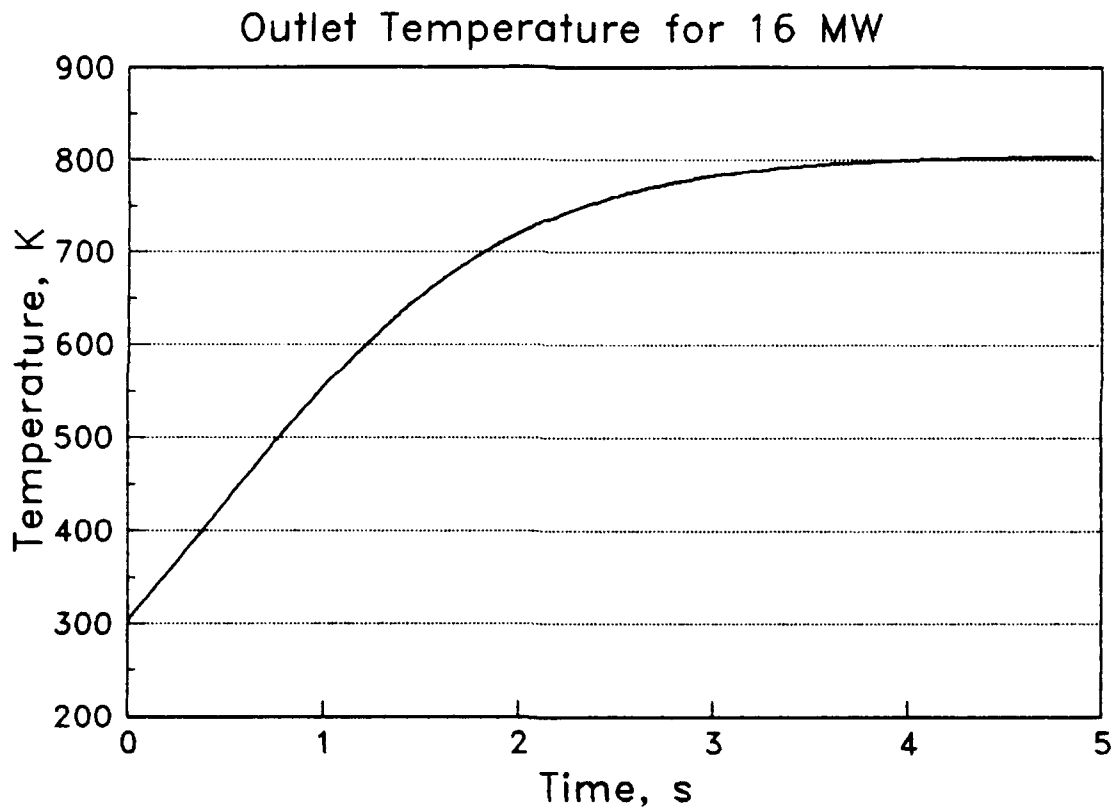


Figure 4. Outlet Temperature for Base Case

Since the fuelbed has been divided into 25 hydrodynamic volumes, the average temperature of the hydrogen can be found in each of these volumes. Figure 5 tracks this average

temperature as the hydrogen flows radially inward for each of the five axial sections.

## Temperature of Axial Segments

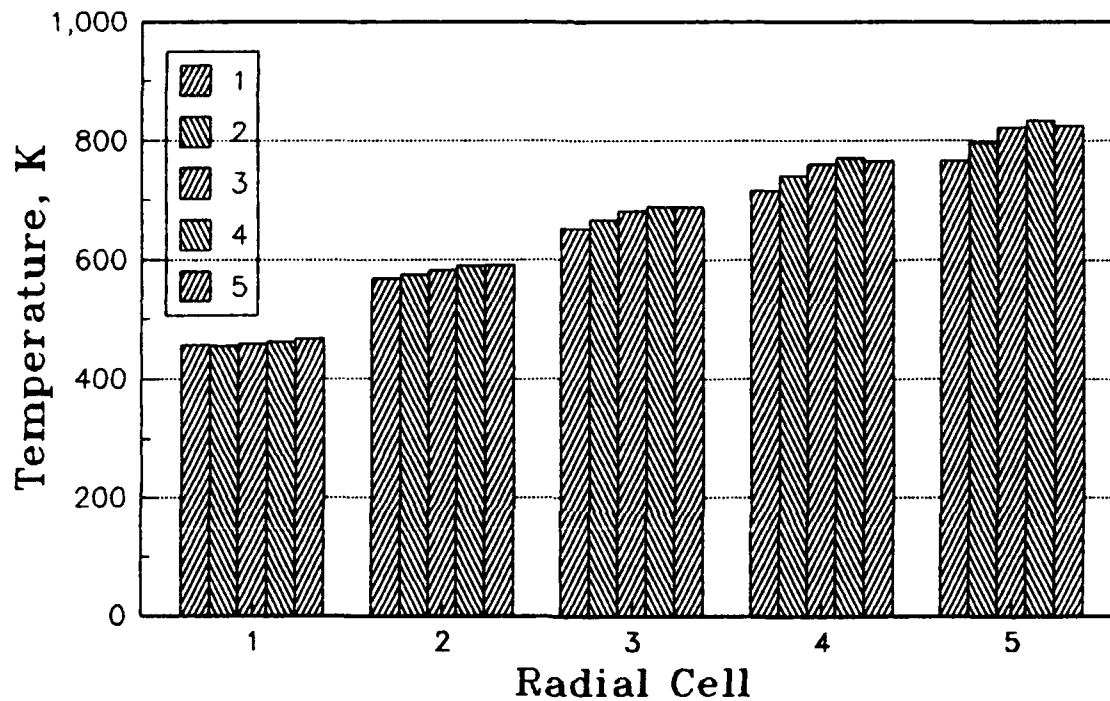


Figure 5. Temperature Profile of Base Case

Each line represents one axial section. The maximum temperature is at the innermost radial section. However, this innermost temperature is not the same for each section. It is highest for section four and lowest for section one, the section nearest the inlet. This inequality is indicative of the nonuniform power distribution through the fuel bed. This could be improved by adjusting the flow rate of

hydrogen. This is accomplished by varying the porosity of the cold frit. At the inlet, the frit could be made less porous thus decreasing the flow rate and increasing the temperature. Likewise, it could be made more porous at the center and lower the temperature in those sections.

As the hydrogen flows through the fuel bed, its velocity increases as it is heated. The velocity of the hydrogen ranges from 0.35 m/s at the outer edge of the fuelbed to 1.7 m/s as it reaches the hot frit.

#### 4.2 Constant Pressure Drop

The first parameter studied was the effect of reactor power on the outlet temperature while the fuelpipe maintained a constant pressure drop. As in the baseline case, the inlet pressure was maintained at 2.068 MPa and the outlet pressure was 2.02 MPa. This pressure drop allowed a hydrogen flow rate of approximately 0.03 kg/s. As the reactor power increased, this flow rate dropped slightly but all flow rates were within 10% of this value. Figure 6 shows the outlet temperature as the reactor power varies from 2 MW to 84 MW. This figure clearly shows a linear relationship between reactor power and outlet temperature. However, the thermal property data generated by the ATHENA code is valid only to 1800 K (Tolli, 1991). Even if the values generated by ATHENA approximate those of an ideal gas at the higher

temperatures, hydrogen begins to depart from this. Dissociation begins at 2800 K for this pressure and increases as the temperature increases (Jahn, 1968:97). Because of these difficulties, the rest of this study will be limited to cases with outlet temperatures below 1800 K. For any future study to be meaningful, data for ranges up to 3500 K will be required.

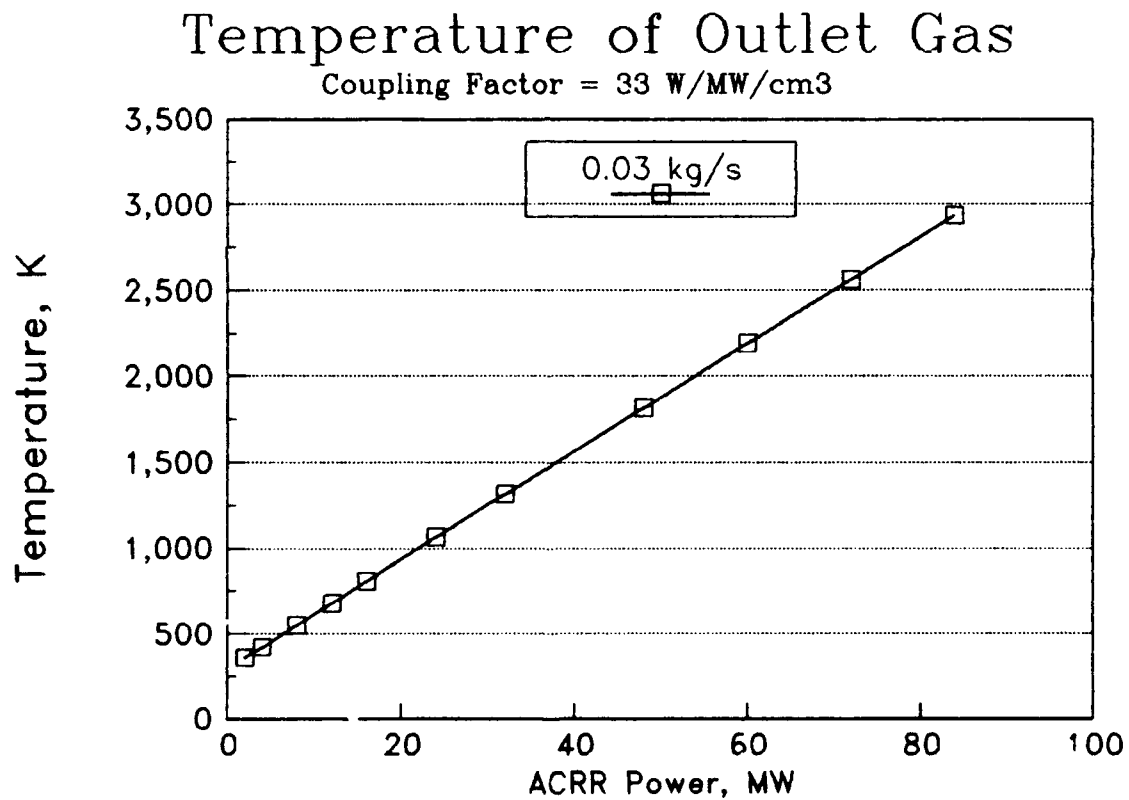


Figure 6. Temperature Comparison at Low Flow



#### 4.3 Higher Pressure Drop

The same reactor power levels were next examined with a larger pressure drop across the pipe. The inlet pressure was kept at 2.068 MPa while the outlet pressure was dropped from 2.02 MPa to 1.85 MPa. This produced a hydrogen flow rate of approximately 0.065 kg/s. While the pressure drop increased by 4.5 times, the mass flow rate only slightly more than doubled. The outlet temperatures for different reactor levels are shown in Figure 7.

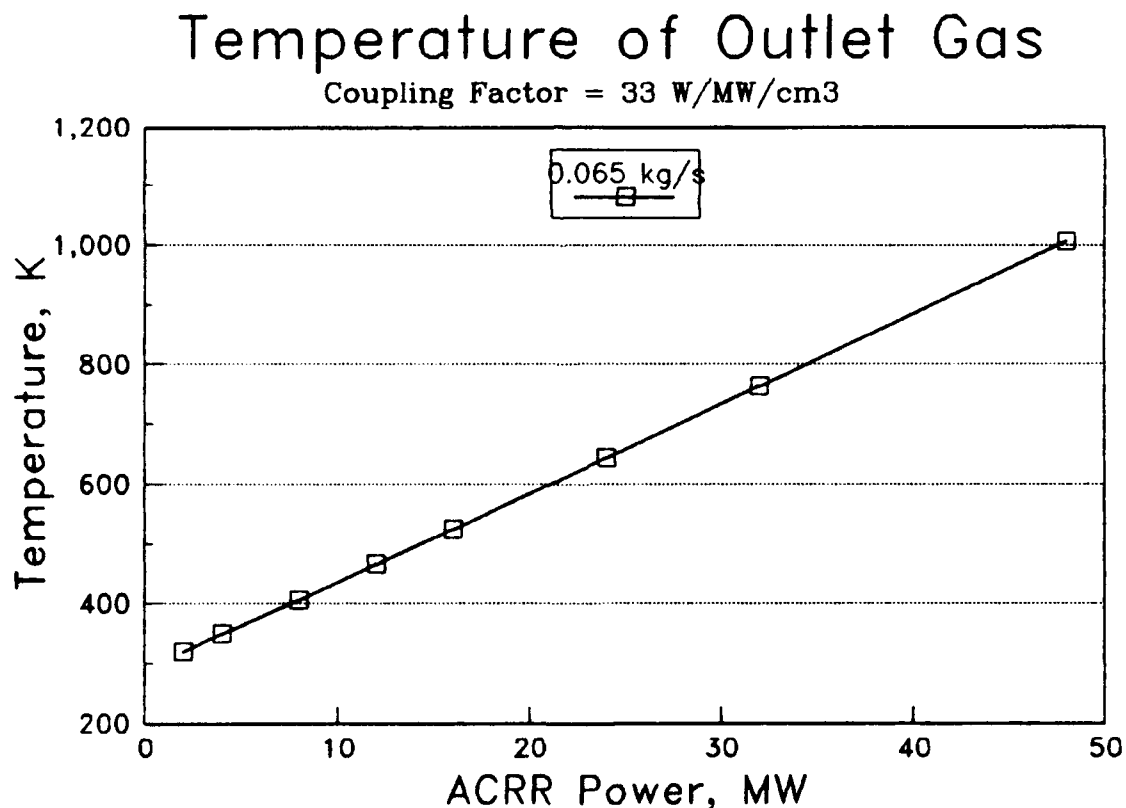


Figure 7. Temperature Comparison at High Flow

The same linear relationship is seen in this figure as in that of the lower flow rate. The only difference is a lower outlet temperature. A direct comparison is shown in Figure 8. Remembering that the initial inlet temperature is 300 K, there is little difference at the lower power levels but this difference is clear at the higher power levels.

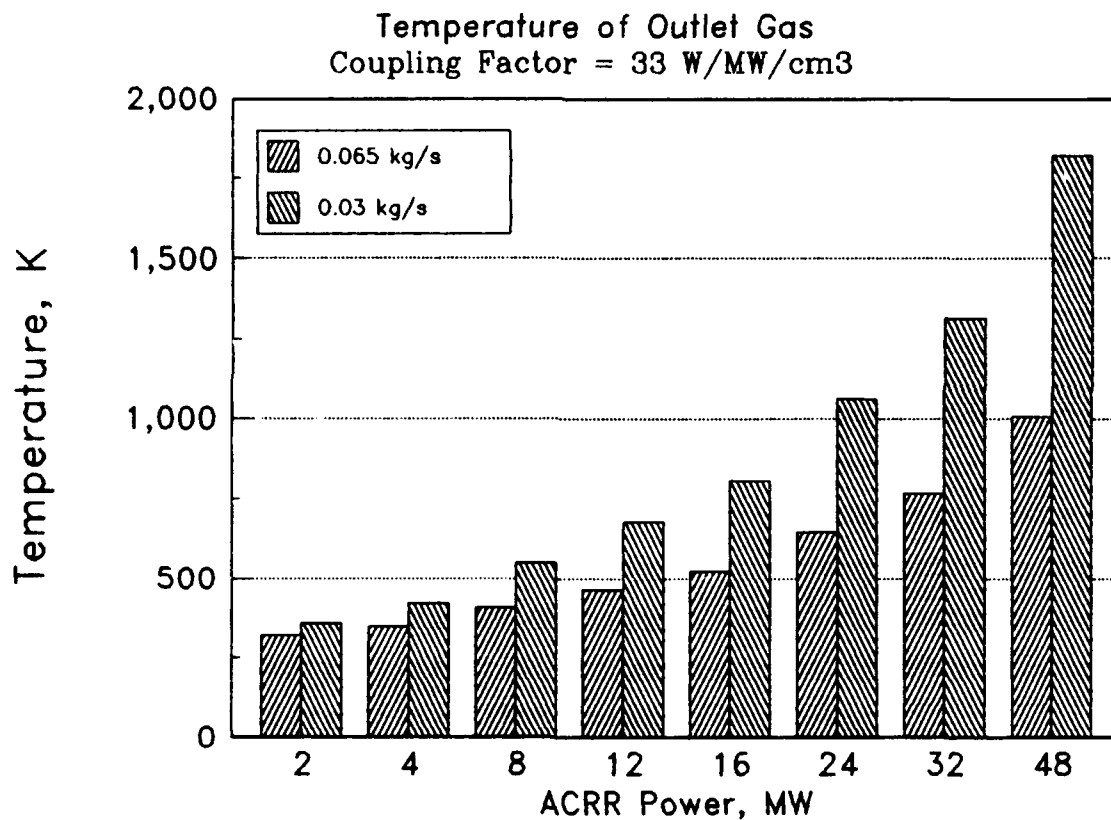


Figure 8. Comparison of Outlet Temperatures at Both Flow Rates

#### 4.4 Coupling Factor

The coupling factor was initially assumed to be 33 W/MW/cm<sup>3</sup>. Assuming the ACRR power level is 16 MW, then 0.23 MW is developed in the fuelpipe (ACRR power x coupling factor x bed volume). By changing the coupling factor, a different power level is assumed to be developed in the fuelpipe. Table 4 shows the different outlet temperatures reached with coupling factors of 30, 33 and 36 W/MW/cm<sup>3</sup>. By changing the coupling factor 9%, the outlet temperature changes by only 6%. The change is linear since the same effect could be observed by changing the ACRR power the same amount. However, this does show that the outlet temperature is somewhat sensitive to some of the initial assumptions.

Table 4

Observed Outlet Temperature for  
Change in Coupling Factor

Coupling Factor	Outlet Temperature
30	757.6
33	804.4
36	851.0

#### 4.5 Mass Flow Rate

The final parameter studied was the mass flow rate. This is related to the variation in the pressure drop but it was earlier shown that this is not a one to one relationship. The inlet pressure was held constant at 2.068 MPa and the outlet pressure was varied from 1.80 MPa to 2.04 MPa at a constant ACRR power of 16 MW. Figure 9 shows the effect of pressure drop on the hydrogen flow rate. Flow rate is clearly not a linear function of pressure drop. As the pressure drop increases, a greater change is required to obtain the same change in hydrogen flow rate.

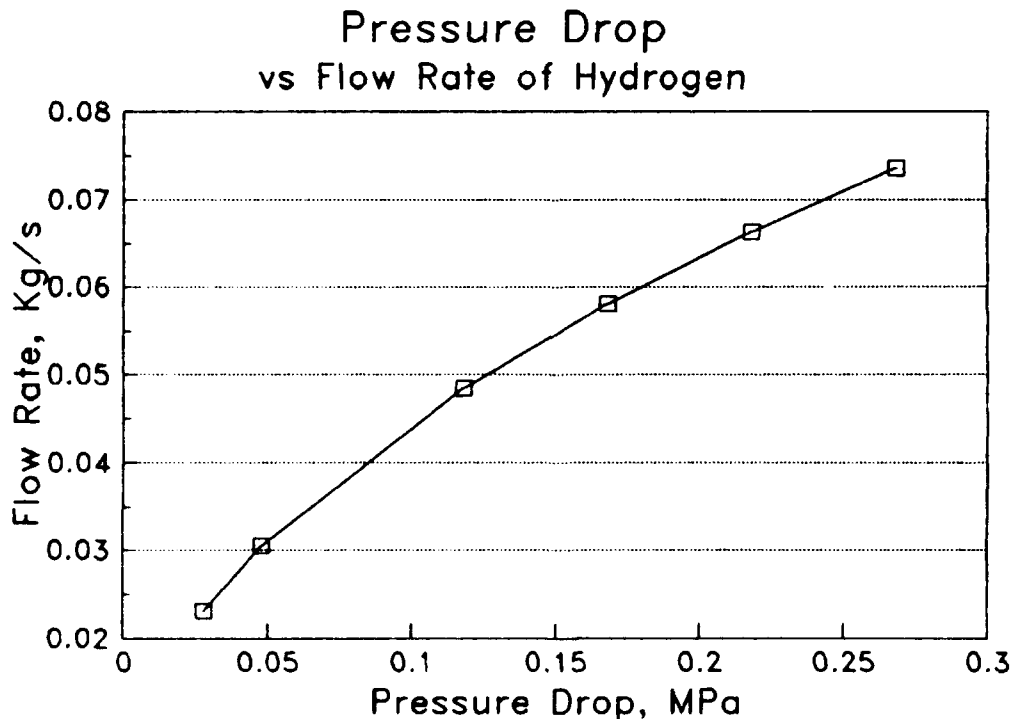


Figure 9. Pressure Drop vs. Flow Rate

The hydrogen cross flow or the flow of hydrogen axially instead of radially was also examined. This cross flow occurs because of pressure differences in the pipe caused by nonuniform heating. Figure 10 shows the maximum cross flow occurs in the outermost radial section which is shown as the first group of bars. Each bar represents the flow between neighboring axial volumes. The negative value for the fourth junction indicates flow going the opposite direction. As the hydrogen flows radially inward, there is less cross flow. It was found that this cross flow varies between one tenth and one percent of the radial flow with the average being three tenths of one percent. As mentioned previously, a non-uniform cold frit could be used to vary the radial flow to obtain a constant outlet temperature. While hydrogen cross flow will occur, its small value should not completely counter-act the use of the cold frit.

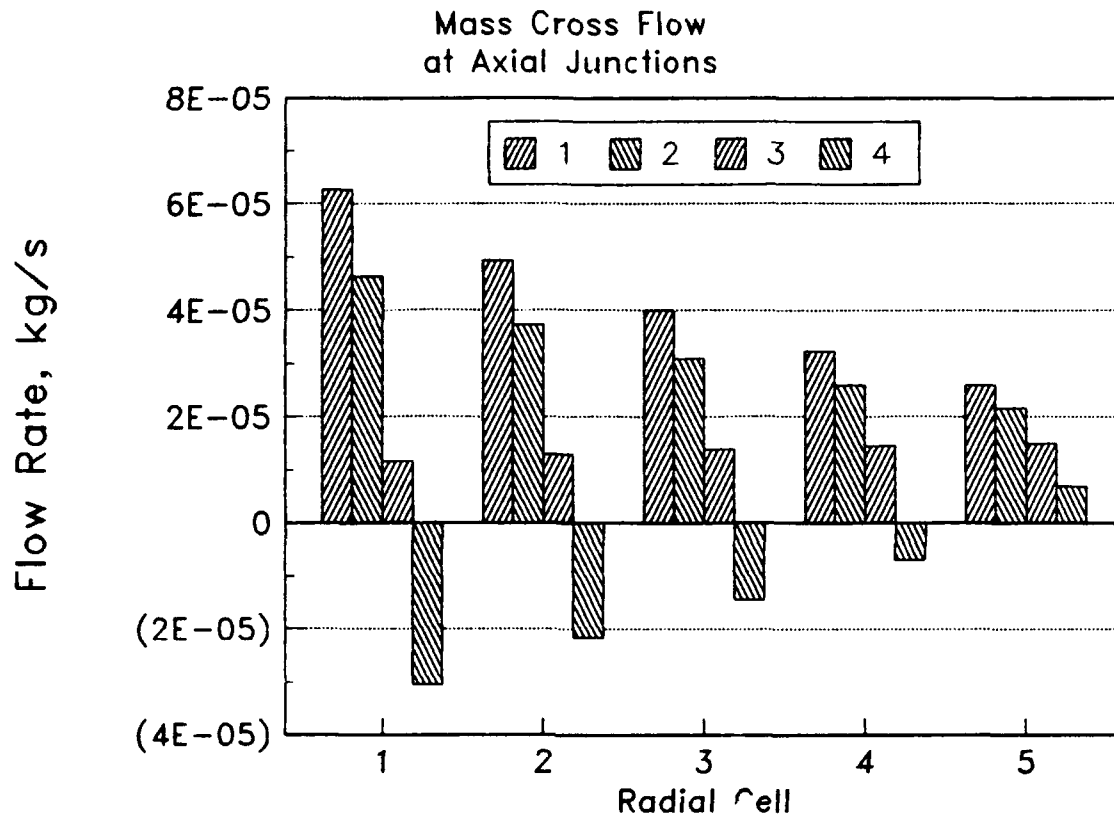


Figure 10. Mass Cross Flow at Axial Junctions

It has been shown that the outlet temperature changes linearly with the hydrogen flow rate. Therefore, it is expected the outlet temperature will be nonlinear with respect to pressure drop as was the hydrogen flow rate. This is shown in Figure 11.

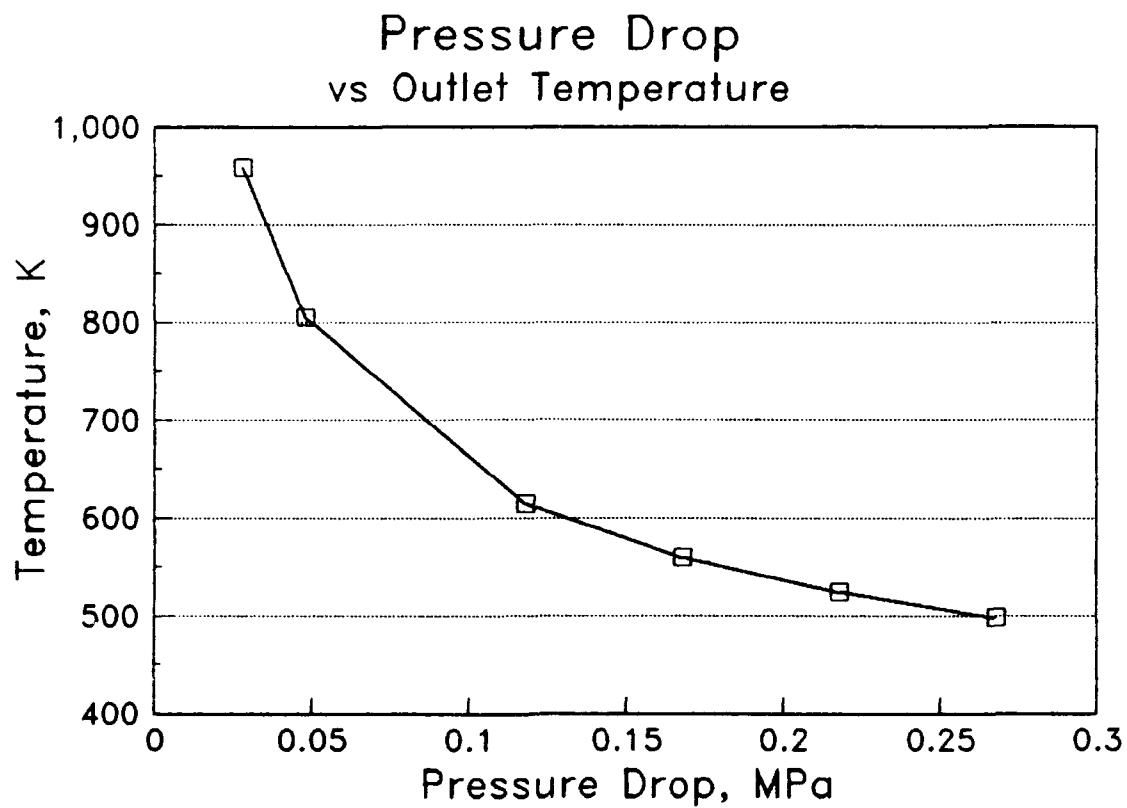


Figure 11. Outlet Temperature vs. Flow Rate

## V Conclusions and Recommendations

It is clear the temperature of the outlet gas is linearly related to the power generated in the particle bed reactor. However, at temperatures above 2800 K, this relation is questioned. Without more complete data concerning the dissociation of hydrogen, further simulations will be meaningless.

The fuelpipe reaches thermal equilibrium within five seconds. This short equilibrium time allows computer simulations to be completed within a reasonable time of twenty four hours.

It was also found that hydrogen flow rate and thus outlet temperature, is not linear with the pressure drop across the fuelpipe. As the pressure drop increases, a smaller increase in hydrogen flow is realized.

The crossflow or axial flow of hydrogen in the fuelpipe averaged just three tenths of one percent of the radial flow. This minimal cross flow should not counter-act the use of a non-uniform cold frit to obtain constant outlet temperatures.

The input deck that has been produced by this thesis work is a starting point for modeling any other fuel pipes. With added information, this could be very useful in simulating the thermal hydraulic characteristics of any fuelpipe.



## Appendix A: Graphics Strip Program

\*This program strips specific data from the run file and  
\*puts it into a usable format.

\*

=fuel strip problem

0000100 strip fmtout

103 0

1002 tempg 060010000

1003 tempg 001010000

1004 tempg 002010000

1005 tempg 005010000

1006 tempg 006010000

1007 tempg 010010000

1008 tempg 011010000

1009 tempg 015010000

1010 tempg 016010000

1013 tempg 025010000

1015 tempg 026010000

1016 tempg 030010000

1017 tempg 031010000

1018 tempg 035010000

1019 tempg 0620 0000

1020 p 001010000

1021 p 015010000

1022 p 035010000

1023 mflowj 236000000

. end of case

## Appendix B: Graphics Modification Program

'This is a program to read the data file produced by Relap5

'All blank lines at the top of the file must be removed

INPUT "File to read: ", file1\$

filename\$ = "c:\tk\" + LEFT\$(file1\$, 6)

'INPUT "Enter drive and directory to store data: ", filename\$

INPUT "Does a new directory need to be made?", Qu\$

IF UCASE\$(Qu\$) = "Y" THEN MKDIR filename\$

OPEN file1\$ FOR INPUT AS #1

LINE INPUT #1, header1\$

LINE INPUT #1, header2\$

LINE INPUT #1, header3\$

INPUT #1, numvar, stuff

numvar = numvar - 1

INPUT #1, junk\$

REDIM title\$(numvar)

REDIM data\$(numvar)

FOR i = 1 TO numvar

    INPUT #1, title\$(i)

NEXT i

INPUT #1, junk\$

REDIM volume\$(numvar)

FOR i = 1 TO numvar

    INPUT #1, volume\$(i)

```

NEXT i
a$ = "0"
FOR i = 1 TO numvar
    IF LEN(volume$(i)) > 9 THEN
        PRINT "Variables named wrong.  Check input file."
        STOP
    END IF
    DO UNTIL LEN(volume$(i)) = 9
        volume$(i) = a$ + volume$(i)
    LOOP
NEXT i
FOR i = 1 TO numvar
    data$(i) = filename$ + "\" + title$(i) + "." + LEFT$(volume$(i), 3)
NEXT i
FOR i = 1 TO numvar
    REDIM value(i, 500)
NEXT i
jcount = 0
DO UNTIL EOF(1)
    jcount = jcount + 1
    junk$ = INPUT$(9, #1)
    FOR i = 1 TO numvar
        INPUT #1, value(i, jcount)      'Check redim of
value(i, j)

```

```
        NEXT i
    LOOP
    FOR i = 1 TO numvar
        OPEN data$(i) FOR OUTPUT AS #2
        FOR k = 1 TO jcount
            WRITE #2, value(i, k)
        NEXT k
        CLOSE #2
    NEXT i
```

## Appendix C: Sample Input File

**\*This is a typical ATHENA input file to model a fuelpipe.**

\*(Carlson and others, 1990).

\*Based on the layout in Figure 3, hydrogen flows from a time

\*dependent volume to an inlet channel and then radially

**inward**

\*through the  $\text{UC}_2$  fuel. It then flows to the exhaust channel

\*at the inside of the annulus.

**\***

=PIPE TEST LOOP Ver 1.0

\*Title input

\*Power of 16 MW ACRR

Pout=1.85e6 0000100

```
newath transnt 101 run
```

**\*Minor edit requests are used to extract information**

\*at different time intervals during the simulation

301 p 060010000

302 p 001010000

303 p 002010000

304 p 003010000

305 p 004010000

306 p 005010000

307 p 006010000

308 p 007010000

309 p 008010000

310 p 009010000

311 p 010010000

312 p 011010000  
313 p 012010000  
314 p 013010000  
315 p 014010000  
316 p 015010000  
317 p 015010000  
318 p 016010000  
319 p 017010000  
320 p 018010000  
321 p 019010000  
322 p 020010000  
323 p 021010000  
324 p 022010000  
325 p 023010000  
326 p 024010000  
327 p 025010000  
328 p 026010000  
329 p 027010000  
330 p 028010000  
331 p 029010000  
332 p 030010000  
333 p 031010000  
334 p 032010000  
335 p 033010000  
336 p 034010000

337 p 035010000  
338 p 062010000  
339 tempg 060010000  
340 tempg 001010000  
341 tempg 002010000  
342 tempg 003010000  
343 tempg 004010000  
344 tempg 005010000  
345 tempg 006010000  
346 tempg 007010000  
347 tempg 008010000  
348 tempg 009010000  
349 tempg 010010000  
350 tempg 011010000  
351 tempg 012010000  
352 tempg 013010000  
353 tempg 014010000  
354 tempg 015010000  
355 tempg 015010000  
356 tempg 016010000  
357 tempg 017010000  
358 tempg 018010000  
359 tempg 019010000  
360 tempg 020010000  
361 tempg 021010000



362 tempg 022010000  
363 tempg 023010000  
364 tempg 024010000  
365 tempg 025010000  
366 tempg 026010000  
367 tempg 027010000  
368 tempg 028010000  
369 tempg 029010000  
370 tempg 030010000  
371 tempg 031010000  
372 tempg 032010000  
373 tempg 033010000  
374 tempg 034010000  
375 tempg 035010000  
376 tempg 062010000  
377 mflowj 101000000  
378 mflowj 106000000  
379 mflowj 111000000  
380 mflowj 116000000  
381 mflowj 121000000  
382 mflowj 126000000  
383 mflowj 232000000  
384 mflowj 233000000  
385 mflowj 234000000  
386 mflowj 235000000

387 mflowj 236000000

388 mflowj 206000000

389 mflowj 210000000

390 mflowj 211000000

391 mflowj 215000000

392 mflowj 216000000

393 mflowj 220000000

394 mflowj 221000000

395 mflowj 222000000

396 mflowj 223000000

397 mflowj 224000000

398 mflowj 225000000

**\*Time step control card**

0000201 1.0e-3 1.0e-9 0.000001 1 100 1000 1000

0000202 0.05 1.0e-9 0.000002 1 5000 20000 20000

0000203 0.5 1.0e-9 0.000005 1 5000 20000 20000

0000204 5.0 1.0e-9 0.00001 1 5000 5000 50000

**\*Defining component's by name and type**

0010000 Inlet1 snglvol

0020000 Inlet2 snglvol

0030000 Inlet3 snglvol

0040000 Inlet4 snglvol

0050000 Inlet5 snglvol

0060000 Reg5\_1 snglvol

0070000 Reg4\_1 snglvol

0080000 Reg3\_1 snlvol  
0090000 Reg2\_1 snlvol  
0100000 Reg1\_1 snlvol  
0110000 Reg5\_2 snlvol  
0120000 Reg4\_2 snlvol  
0130000 Reg3\_2 snlvol  
0140000 Reg2\_2 snlvol  
0150000 Reg1\_2 snlvol  
0160000 Reg5\_3 snlvol  
0170000 Reg4\_3 snlvol  
0180000 Reg3\_3 snlvol  
0190000 Reg2\_3 snlvol  
0200000 Reg1\_3 snlvol  
0210000 Reg5\_4 snlvol  
0220000 Reg4\_4 snlvol  
0230000 Reg3\_4 snlvol  
0240000 Reg2\_4 snlvol  
0250000 Reg1\_4 snlvol  
0260000 Reg5\_5 snlvol  
0270000 Reg4\_5 snlvol  
0280000 Reg3\_5 snlvol  
0290000 Reg2\_5 snlvol  
0300000 Reg1\_5 snlvol  
0310000 Outlet5 snlvol  
0320000 Outlet4 snlvol

0330000 Outlet3 snglvol  
0340000 Outlet2 snglvol  
0350000 Outlet1 snglvol  
\*Define junctions  
1010000 inbdy sngljun  
1020000 to2 sngljun  
1030000 to3 sngljun  
1040000 to4 sngljun  
1050000 to5 sngljun  
1060000 to5\_1 sngljun  
1070000 to4\_1 sngljun  
1080000 to3\_1 sngljun  
1090000 to2\_1 sngljun  
1100000 to1\_1 sngljun  
1110000 to5\_2 sngljun  
1120000 to4\_2 sngljun  
1130000 to3\_2 sngljun  
1140000 to2\_2 sngljun  
1150000 to1\_2 sngljun  
1160000 to5\_3 sngljun  
1170000 to4\_3 sngljun  
1180000 to3\_3 sngljun  
1190000 to2\_3 sngljun  
1200000 to1\_3 sngljun  
1210000 to5\_4 sngljun

1220000 to4\_4 sngl jun  
1230000 to3\_4 sngl jun  
1240000 to2\_4 sngl jun  
1250000 to1\_4 sngl jun  
1260000 to5\_5 sngl jun  
1270000 to4\_5 sngl jun  
1280000 to3\_5 sngl jun  
1290000 to2\_5 sngl jun  
1300000 to1\_5 sngl jun  
1310000 toOut5 sngl jun  
1320000 toOut4 sngl jun  
1330000 toOut3 sngl jun  
1340000 toOut2 sngl jun  
1350000 toOut1 sngl jun  
2320000 toExh4 sngl jun  
2330000 toExh3 sngl jun  
2340000 toExh2 sngl jun  
2350000 toExh1 sngl jun  
2360000 toExit sngl jun  
\*These are the cross flow junctions  
2060000 toV6 sngl jun  
2070000 toV7 sngl jun  
2080000 toV8 sngl jun  
2090000 toV9 sngl jun  
2100000 toV10 sngl jun

```

2110000 toV11 snljun
2120000 toV12 snljun
2130000 toV13 snljun
2140000 toV14 snljun
2150000 toV15 snljun
2160000 toV16 snljun
2170000 toV17 snljun
2180000 toV18 snljun
2190000 toV19 snljun
2200000 toV20 snljun
2210000 toV21 snljun
2220000 toV22 snljun
2230000 toV23 snljun
2240000 toV24 snljun
2250000 toV25 snljun
0600000 Enter tmdpvol
0620000 Exit tmdpvol
*Geometry input for control volumes
*Inlet Annulus
0010101 3.408e-3 5.080e-2 0. 0. 0. 0. 0. 2.908e-2 11100
0020101 3.408e-3 5.080e-2 0. 0. 0. 0. 0. 2.908e-2 11100
0030101 3.408e-3 5.080e-2 0. 0. 0. 0. 0. 2.908e-2 11100
0040101 3.408e-3 5.080e-2 0. 0. 0. 0. 0. 2.908e-2 11100
0050101 3.408e-3 5.080e-2 0. 0. 0. 0. 0. 2.908e-2 11100
*Bed, Region 5 (outer ring)

```

\*rH=1/6\*e/(1-e)\*D for a packed bed

\*DH=2\*rH

0060101 3.028e-3 2.520e-3 0. 0. 0. 0. 0. 94.8e-6 11110

0110101 3.028e-3 2.520e-3 0. 0. 0. 0. 0. 94.8e-6 11110

0160101 3.028e-3 2.520e-3 0. 0. 0. 0. 0. 94.8e-6 11110

0210101 3.028e-3 2.520e-3 0. 0. 0. 0. 0. 94.8e-6 11110

0260101 3.028e-3 2.520e-3 0. 0. 0. 0. 0. 94.8e-6 11110

\*Bed, Region 4

0070101 0. 2.520e-3 6.9003e-6 0. 0. 0. 0. 94.8e-6 11110

0120101 0. 2.520e-3 6.9003e-6 0. 0. 0. 0. 94.8e-6 11110

0170101 0. 2.520e-3 6.9003e-6 0. 0. 0. 0. 94.8e-6 11110

0220101 0. 2.520e-3 6.9003e-6 0. 0. 0. 0. 94.8e-6 11110

0270101 0. 2.520e-3 6.9003e-6 0. 0. 0. 0. 94.8e-6 11110

\*Bed, Region 3

0080101 0. 2.520e-3 6.1706e-6 0. 0. 0. 0. 94.8e-6 11110

0130101 0. 2.520e-3 6.1706e-6 0. 0. 0. 0. 94.8e-6 11110

0180101 0. 2.520e-3 6.1706e-6 0. 0. 0. 0. 94.8e-6 11110

0230101 0. 2.520e-3 6.1706e-6 0. 0. 0. 0. 94.8e-6 11110

0280101 0. 2.520e-3 6.1706e-6 0. 0. 0. 0. 94.8e-6 11110

\*Bed, Region 2

0090101 0. 2.520e-3 5.4409e-6 0. 0. 0. 0. 94.8e-6 11110

0140101 0. 2.520e-3 5.4409e-6 0. 0. 0. 0. 94.8e-6 11110

0190101 0. 2.520e-3 5.4409e-6 0. 0. 0. 0. 94.8e-6 11110

0240101 0. 2.520e-3 5.4409e-6 0. 0. 0. 0. 94.8e-6 11110

0290101 0. 2.520e-3 5.4409e-6 0. 0. 0. 0. 94.8e-6 11110

**\*Bed, Region 1**

0100101 0. 2.520e-3 4.7112e-6 0. 0. 0. 0. 94.8e-6 11110  
0150101 0. 2.520e-3 4.7112e-6 0. 0. 0. 0. 94.8e-6 11110  
0200101 0. 2.520e-3 4.7112e-6 0. 0. 0. 0. 94.8e-6 11110  
0250101 0. 2.520e-3 4.7112e-6 0. 0. 0. 0. 94.8e-6 11110  
0300101 0. 2.520e-3 4.7112e-6 0. 0. 0. 0. 94.8e-6 11110

**\*Exhaust Channel**

0310101 6.379e-4 5.080e-2 0. 0. 0. 0. 0. 2.850e-2 11100  
0320101 6.379e-4 5.080e-2 0. 0. 0. 0. 0. 2.850e-2 11100  
0330101 6.379e-4 5.080e-2 0. 0. 0. 0. 0. 2.850e-2 11100  
0340101 6.379e-4 5.080e-2 0. 0. 0. 0. 0. 2.850e-2 11100  
0350101 6.379e-4 5.080e-2 0. 0. 0. 0. 0. 2.850e-2 11100

**\*Geometry input for single junction data**

**\*Inlet Annulus**

1010101 060000000 001000000 3.408e-3 0. 0. 031020 1.0 1.0  
1020101 001010000 002000000 3.408e-3 0. 0. 031020 1.0 1.0  
1030101 002010000 003000000 3.408e-3 0. 0. 031020 1.0 1.0  
1040101 003010000 004000000 3.408e-3 0. 0. 031020 1.0 1.0  
1050101 004010000 005000000 3.408e-3 0. 0. 031020 1.0 1.0

**\*Bed Inlet Thru Cold Frit**

1060101 001010000 006000000 9.587e-3 3.882e5 0. 031022 1.0  
1.0  
1110101 002010000 011000000 9.587e-3 3.112e5 0. 031022 1.0  
1.0  
1160101 003010000 016000000 9.587e-3 2.999e5 0. 031022 1.0



1.0  
 1210101 004010000 021000000 9.587e-3 3.302e5 0. 031022 1.0  
 1.0  
 1260101 005010000 026000000 9.587e-3 4.226e5 0. 031022 1.0  
 1.0  
 \*to Bed Radial 4  
 1070101 006010000 007000000 7.979e-3 1319.0 0. 031020 1.0  
 1.0  
 1120101 011010000 012000000 7.979e-3 1221.0 0. 031020 1.0  
 1.0  
 1170101 016010000 017000000 7.979e-3 1193.0 0. 031020 1.0  
 1.0  
 1220101 021010000 022000000 7.979e-3 1215.0 0. 031020 1.0  
 1.0  
 1270101 026010000 027000000 7.979e-3 1293.0 0. 031020 1.0  
 1.0  
 \*to Bed radial 3  
 1080101 007010000 008000000 7.183e-3 1178.0 0. 031020 1.0  
 1.0  
 1130101 012010000 013000000 7.183e-3 1086.0 0. 031020 1.0  
 1.0  
 1180101 017010000 018000000 7.183e-3 1062.0 0. 031020 1.0  
 1.0  
 1230101 022010000 023000000 7.183e-3 1080.0 0. 031020 1.0  
 1.0

1280101 027010000 028000000 7.183e-3 1153.0 0. 031020 1.0  
1.0

\*to Bed Radial 2

1090101 008010000 009000000 6.385e-3 1126.0 0. 031020 1.0  
1.0

1140101 013010000 014000000 6.385e-3 1039.0 0. 031020 1.0  
1.0

1190101 018010000 019000000 6.385e-3 1013.0 0. 031020 1.0  
1.0

1240101 023010000 024000000 6.385e-3 1032.0 0. 031020 1.0  
1.0

1290101 028010000 029000000 6.385e-3 1103.0 0. 031020 1.0  
1.0

\*To Bed Radial 1

1100101 009010000 010000000 5.588e-3 1060.0 0. 031020 1.0  
1.0

1150101 014010000 015000000 5.588e-3 979.0 0. 031020 1.0 1.0

1200101 019010000 020000000 5.588e-3 956.0 0. 031020 1.0 1.0

1250101 024010000 025000000 5.588e-3 973.0 0. 031020 1.0 1.0

1300101 029010000 030000000 5.588e-3 1039.0 0. 031020 1.0  
1.0

\*To Bed Outlet thru Hot frit

1310101 030010000 031000000 4.791e-3 431.0 0. 031021 1.0 1.0

1320101 025010000 032000000 4.791e-3 405.0 0. 031021 1.0 1.0

1330101 020010000 033000000 4.791e-3 399.0 0. 031021 1.0 1.0

1340101 015010000 034000000 4.791e-3 408.0 0. 031021 1.0 1.0

1350101 010010000 035000000 4.791e-3 440.0 0. 031021 1.0 1.0

**\*Hot Channel**

2320101 031010000 032000000 6.379e-4 0. 0. 31020 1.0 1.0

2330101 032010000 033000000 6.379e-4 0. 0. 31020 1.0 1.0

2340101 033010000 034000000 6.379e-4 0. 0. 31020 1.0 1.0

2350101 034010000 035000000 6.379e-4 0. 0. 31020 1.0 1.0

2360101 035010000 062000000 6.379e-4 0. 0. 31020 1.0 1.0

0600101 3.408e-3 1.0 0.0 0.0 -90.0 -1.0 0.0 0.0 00010

0620101 6.379e-4 1.0 0.0 0.0 90.0 1.0 0.0 0.0 00010

**\*Cross Flows**

2060101 011010000 006000000 0. 1.0e 4 1.0e 4 31023 1.0 1.0

2070101 012010000 007000000 0. 1.0e 4 1.0e 4 31023 1.0 1.0

2080101 013010000 008000000 0. 1.0e 4 1.0e 4 31023 1.0 1.0

2090101 014010000 009000000 0. 1.0e 4 1.0e 4 31023 1.0 1.0

2100101 015010000 010000000 0. 1.0e 4 1.0e 4 31023 1.0 1.0

2110101 016010000 011000000 0. 1.0e 4 1.0e 4 31023 1.0 1.0

2120101 017010000 012000000 0. 1.0e 4 1.0e 4 31023 1.0 1.0

2130101 018010000 013000000 0. 1.0e 4 1.0e 4 31023 1.0 1.0

2140101 019010000 014000000 0. 1.0e 4 1.0e 4 31023 1.0 1.0

2150101 020010000 015000000 0. 1.0e 4 1.0e 4 31023 1.0 1.0

2160101 021010000 016000000 0. 1.0e 4 1.0e 4 31023 1.0 1.0

2170101 022010000 017000000 0. 1.0e 4 1.0e 4 31023 1.0 1.0

2180101 023010000 018000000 0. 1.0e 4 1.0e 4 31023 1.0 1.0

2190101 024010000 019000000 0. 1.0e 4 1.0e 4 31023 1.0 1.0

2200101 025010000 020000000 0. 1.0e 4 1.0e 4 31023 1.0 1.0  
 2210101 026010000 021000000 0. 1.0e 4 1.0e 4 31023 1.0 1.0  
 2220101 027010000 022000000 0 1.0e 4 1.0e 4 31023 1.0 1.0  
 2230101 028010000 023000000 0. 1.0e 4 1.0e 4 31023 1.0 1.0  
 2240101 029010000 024000000 0. 1.0e 4 1.0e 4 31023 1.0 1.0  
 2250101 030010000 025000000 0. 1.0e 4 1.0e 4 31023 1.0 1.0

**\*INITIAL INPUT DATA Pressure and Temperature**

**\*Inlet Annulus**

0010200 303 2.068e 6 300.0  
 0020200 303 2.068e 6 300.0  
 0030200 303 2.068e 6 300.0  
 0040200 303 2.068e 6 300.0  
 0050200 303 2.068e 6 300.0

**\*Bed, Region 5 (Outer ring)**

0060200 303 2019000.0 300.0  
 0110200 303 2021000.0 300.0  
 0160200 303 2021000.0 300.0  
 0210200 303 2021000.0 300.0  
 0260200 303 2021000.0 300.0

**\*Bed, Region 4**

0070200 303 2018000.0 300.0  
 0120200 303 2020000.0 300.0  
 0170200 303 2021000.0 300.0  
 0220200 303 2021000.0 300.0  
 0270200 303 2020000.0 300.0

**\*Bed, Region 3**

0080200 303 2017000.0 300.0

0130200 303 2018000.0 300.0

0180200 303 2019000.0 300.0

0230200 303 2019000.0 300.0

0280200 303 2018000.0 300.0

**\*Bed, Region 2**

0090200 303 2017000.0 300.0

0140200 303 2018000.0 300.0

0190200 303 2019000.0 300.0

0240200 303 2019000.0 300.0

0290200 303 2018000.0 300.0

**\*Bed, Region 1**

0100200 303 2017000.0 300.0

0150200 303 2017000.0 300.0

0200200 303 2018000.0 300.0

0250200 303 2018000.0 300.0

0300200 303 2017000.0 300.0

**\*Exhaust Channel**

0310200 303 2016000.0 300.0

0320200 303 2016000.0 300.0

0330200 303 2016000.0 300.0

0340200 303 2016000.0 300.0

0350200 303 2016000.0 300.0

0600200 303

0600201 0.0 2.068e 6 300.0

0620200 303

0620201 0.0 1.85e 6 300.0

\*Initial input data for junctions mass flow rates

1010201 1 0. 0.032 0.

1020201 1 0. 0.0259 0.

1030201 1 0. 0.0191 0.

1040201 1 0. 0.0123 0.

1050201 1 0. 0.00579 0.

1060201 1 0. 0.00616 0.

1070201 1 0. 0.00616 0.

1080201 1 0. 0.00616 0.

1090201 1 0. 0.00616 0.

1100201 1 0. 0.00616 0.

1110201 1 0. 0.00674 0.

1120201 1 0. 0.00674 0.

1130201 1 0. 0.00674 0.

1140201 1 0. 0.00674 0.

1150201 1 0. 0.00674 0.

1160201 1 0. 0.00684 0.

1170201 1 0. 0.00684 0.

1180201 1 0. 0.00684 0.

1190201 1 0. 0.00684 0.

1200201 1 0. 0.00684 0.

1210201 1 0. 0.00649 0.  
1220201 1 0. 0.00649 0.  
1230201 1 0. 0.00649 0.  
1240201 1 0. 0.00649 0.  
1250201 1 0. 0.00649 0.  
1260201 1 0. 0.00579 0.  
1270201 1 0. 0.00579 0.  
1280201 1 0. 0.00579 0.  
1290201 1 0. 0.00579 0.  
1300201 1 0. 0.00579 0.  
1310201 1 0. 0.00579 0.  
1320201 1 0. 0.00649 0.  
1330201 1 0. 0.00684 0.  
1340201 1 0. 0.00674 0.  
1350201 1 0. 0.00616 0.  
2320201 1 0. 0.00579 0.  
2330201 1 0. 0.0123 0.  
2340201 1 0. 0.0191 0.  
2350201 1 0. 0.0259 0.  
2360201 1 0. 0.032 0.

**\*Cross Flow Data**

2060201 1 0. 0. 0.  
2070201 1 0. 0. 0.  
2080201 1 0. 0. 0.  
2090201 1 0. 0. 0.

2100201 1 0. 0. 0.

2110201 1 0. 0. 0.

2120201 1 0. 0. 0.

2130201 1 0. 0. 0.

2140201 1 0. 0. 0.

2150201 1 0. 0. 0.

2160201 1 0. 0. 0.

2170201 1 0. 0. 0.

2180201 1 0. 0. 0.

2190201 1 0. 0. 0.

2200201 1 0. 0. 0.

2210201 1 0. 0. 0.

2220201 1 0. 0. 0.

2230201 1 0. 0. 0.

2240201 1 0. 0. 0.

2250201 1 0. 0. 0.

\*\*\*\*\*Heat structure data\*\*\*\*\*

\*Bed Radial Region #5

10061000 5 5 3 1 0.0 0 0 8

10061100 0 1

10061101 1 1.2e-4

\*Fuel particle geometry

10061102 1 1.52e-4

10061103 1 2.02e-4

10061104 1 2.5e-4

10061201 111 1

\*kernel





10071201 111 1 \*kernel  
 10071202 222 2 \*buffer  
 10071203 333 3 \*LTI  
 10071204 444 4 \*coating  
 10071301 1.0 1  
 10071302 0.0 2  
 10071303 0.0 3  
 10071304 0.0 4  
 10071400 0  
 10071401 1000.0 5  
 10071501 0 0 0 0 0.0 5  
 10071601 007010000 5000000 1 0 0.1472 5  
 10071701 006 1.0963 0.0 0.0 1  
 10071702 006 1.2210 0.0 0.0 2  
 10071703 006 1.2613 0.0 0.0 3  
 10071704 006 1.2304 0.0 0.0 4  
 10071705 006 1.1260 0.0 0.0 5  
 10071801 0.0 10.0 10.0 10.0 10.0 1.0 1.0 2.0 5  
 10071901 0.0 10.0 10.0 10.0 10.0 1.0 1.0 2.0 5  
 \*Bed Radial Region #3  
 10081000 5 5 3 1 0.0 0 0 8  
 10081100 0 1  
 10081101 1 1.2e-4  
 10081102 1 1.52e-4  
 10081103 1 2.02e-4

10081104 1 2.5e-4  
 10081201 111 1 \*kernel  
 10081202 222 2 \*buffer  
 10081203 333 3 \*LTI  
 10081204 444 4 \*coating  
 10081301 1.0 1  
 10081302 0.0 2  
 10081303 0.0 3  
 10081304 0.0 4  
 10081400 0  
 10081401 1000.0 5  
 10081501 0 0 0 0 0.0 5  
 10081601 008010000 5000000 1 0 0.1316 5  
 10081701 006 0.8506 0.0 0.0 1  
 10081702 006 0.9473 0.0 0.0 2  
 10081703 006 0.9787 0.0 0.0 3  
 10081704 006 0.9547 0.0 0.0 4  
 10081705 006 0.8737 0.0 0.0 5  
 10081801 0.0 10.0 10.0 10.0 10.0 1.0 1.0 2.0 5  
 10081901 0.0 10.0 10.0 10.0 10.0 1.0 1.0 2.0 5  
 \*Bed Radial Region #2  
 10091000 5 5 3 1 0.0 0 0 8  
 10091100 0 1  
 10091101 1 1.2e-4  
 10091102 1 1.52e-4

10091103 1 2.02e-4  
 10091104 1 2.5e-4  
 10091201 111 1 \*kernel  
 10091202 222 2 \*buffer  
 10091203 333 3 \*LTI  
 10091204 444 4 \*coating  
 10091301 1.0 1  
 10091302 0.0 2  
 10091303 0.0 3  
 10091304 0.0 4  
 10091400 0  
 10091401 1000.0 5  
 10091501 0 0 0 0 0.0 5  
 10091601 009010000 5000000 1 0 0.1161 5  
 10091701 006 0.6715 0.0 0.0 1  
 10091702 006 0.7478 0.0 0.0 2  
 10091703 006 0.7725 0.0 0.0 3  
 10091704 006 0.7536 0.0 0.0 4  
 10091705 006 0.6896 0.0 0.0 5  
 10091801 0.0 10.0 10.0 10.0 10.0 1.0 1.0 2.0 5  
 10091901 0.0 10.0 10.0 10.0 10.0 1.0 1.0 2.0 5  
 \*Bed Radial Region #1  
 10101000 5 5 3 1 0.0 0 0 8  
 10101100 0 1  
 10101101 1 1.2e-4

10101102 1 1.52e-4  
 10101103 1 2.02e-4  
 10101104 1 2.5e-4  
 10101201 111 1 \*kernel  
 10101202 222 2 \*buffer  
 10101203 333 3 \*LTI  
 10101204 444 4 \*coating  
 10101301 1.0 1  
 10101302 0.0 2  
 10101303 0.0 3  
 10101304 0.0 4  
 10101400 0  
 10101401 1000.0 5  
 10101501 0 0 0 0 0.0 5  
 10101601 010010000 5000000 1 0 0.1005 5  
 10101701 006 0.5311 0.0 0.0 1  
 10101702 006 0.5914 0.0 0.0 2  
 10101703 006 0.6110 0.0 0.0 3  
 10101704 006 0.5960 0.0 0.0 4  
 10101705 006 0.5454 0.0 0.0 5  
 10101801 0.0 10.0 10.0 10.0 10.0 1.0 1.0 2.0 5  
 10101901 0.0 10.0 10.0 10.0 10.0 1.0 1.0 2.0 5  
 \*Material Data Table for Kernel  
 20111100 tbl/fctn 1 1  
 20111101 200.0 14.7

20111102 1000.0 15.0  
 20111103 1600.0 16.5  
 20111104 2200.0 19.4  
 20111105 2600.0 22.2  
 20111106 3200.0 28.1  
 20111151 298.15 2.64e+6  
 20111152 700.0 3.34e+6  
 20111153 1400.0 4.20e+6  
 20111154 2038.0 5.94e+6  
 20111155 2042.0 5.34e+6  
 20111156 2700.0 5.34e+6  
 20111157 3300.0 5.34e+6

**\*Material Data Table for Buffer**

20122200 tbl/fctn 1 1  
 20122201 88.0  
 20122251 1.71e+6

**\*Material Data Table for LTI**

20133300 tbl/fctn 1 1  
 20133301 33.0 \*W/m K  
 20133351 3.72e+6 \*J/m<sup>3</sup> K

**\*Material Data Table for Coating**

20144400 tbl/fctn 1 1  
 20144401 100.0 16.2  
 20144402 200.0 32.4  
 20144403 600.0 32.4

20144404 1000.0 35.5

20144405 2500.0 47.0

20144406 3000.0 47.0

20144407 3500.0 47.0

20144451 298.15 2.35e+6

\*Data from Refractory Carbides, Ed Storms

20144452 300.0 2.37e+6

20144453 500.0 2.99e+6

20144454 900.0 3.15e+6

20144455 1800.0 3.39e+6

20144456 2800.0 4.27e+6

20144457 3200.0 4.79e+6

\*Extrapolated linearly from 3000 K

\*Power General Data Table

20200600 power 0.0 1.0 565.6

20200601 -1.0 16.0

20200602 10.0 16.0

. end of case

### Bibliography

- Araj, K. J. and others. "Ultra High Temperature Direct Propulsion," Transactions of the Fifth Symposium on Space Nuclear Power Systems. 53-60. Malabar, FL: Orbit Book Company, 1988.
- Asker, James R. "Nuclear Rockets Gain Support For Propelling Mars Mission," Aviation Week & Space Technology, 134: 24-25 (March 18, 1991).
- , James R. "Moon/Mars Prospects May Hinge on Nuclear Propulsion," Aviation Week & Space Technology, 134: 38-42 (December 2, 1991).
- Benenati, K. J. and F. L. Horn. "Thermal-Hydraulic Considerations for Particle Bed Reactors," Space Nuclear Power Systems 1987, edited by M. S. El-Genk and M. D. Hoover. Malabar, FL: Orbit Book Co., 1988.
- Bennett, C. O. and J. E. Myers. Momentum, Heat, and Mass Transfer (Third Edition). New York: McGraw-Hill Book Company, 1982).
- Carlson, K. E. and others. RELAP5/MOD3 Code Manual, Volume 2, edited by C. M. Allison and others. Washington: U. S. Nuclear Regulatory Commission, 1990.
- Fletcher, C. D. "Simulation of the Preliminary General Electric SP-100 Space Reactor Concept using the ATHENA Computer Code," Space Nuclear Power Systems 1986, edited by M. S. El-Genk and M. D. Hoover. Malabar, FL: Orbit Book Co., 1987.
- Jahn, Robert G. Physics of Electric Propulsion. New York: McGraw-Hill Book Company, 1968.
- Lazareth, O. W. and others. "Analysis of the Start-up and Control of a Particle Bed Reactor," Space Nuclear Power Systems 1987, edited by M. S. El-Genk and M. D. Hoover. Malabar, FL: Orbit Book Co., 1988.
- Leyse, Carl F. and others. A Preliminary Stage Configuration for a Low Pressure Nuclear Thermal Rocket (LPNTR). AIAA 90-3791. Washington: AIAA, 1990a.
- , Space Nuclear Propulsion - The Low Pressure Nuclear Thermal Rocket. AIAA 90-1952. Washington: AIAA, 1990b.



Ramsthaler, Jack H. And Tal K. Sulmeisters. "Comparison Direct Thrust Nuclear Engine, Nuclear Electric Engine, and a Chemical Engine for Future Space Missions," Transactions of the Fifth Symposium on Space Nuclear Power Systems. 19-22. Malabar, FL: Orbit Book Company, 1988.

Roth, P. A. Space Reactor Fuel Element Analysis Using ATHENA. Unpublished Report. Idaho National Engineering Laboratory, EG&G Idaho Inc., Idaho Falls, ID.

----- . "ATHENA Simulation of the 300-kW SP-100," Space Nuclear Power Systems 1987, edited by M. S. El-Genk and M. D. Hoover. Malabar, FL: Orbit Book Co., 1988.

Smalec, L. M. Technical Data Record for Design Parameters of the Pipe Test Loop for ATHENA Modeling. Document Identifier 12-3000657-00. Babcock & Wilcox, Lynchburg, VA, December 1990.

Storms, Edmund K. The Refractory Carbides. New York: Academic Press, 1967.

"Synthesis Group Panel Backs Nuclear in Space," Nuclear News, 34: 86-89 (August 1991).

Tolli, John. Personal Communication. Idaho National Engineering Laboratory, 16 Dec 1991.

Touloukian, Y. S. and others. Thermophysical Properties of Matter, Volume 2. New York: IFI/Plenum, 1970.

### Vita

Captain Mark J. Dibben was born on 26 April 1963 in Junction City, KS. He graduated from high school there in 1981 before attending the University of Kansas. While there he received his commission through ROTC and graduated with a Bachelor of Science in Chemical Engineering in December 1985. His first assignment was to the Occupational and Environmental Health Laboratory at Brooks AFB, Texas. While there he worked throughout the laboratory supervising and analyzing water, air and soil samples for any occupational or environmental hazards. He entered the School of Engineering, Air Force Institute of Technology, in August 1990.

Permanent Address: 801 W. Elm  
Junction City, Kansas

March 1992

Master's Thesis

MODEL OF A NUCLEAR THERMAL TEST PIPE  
USING ATHENA

Mark J. Dibben, Captain, USAF

Air Force Institute of Technology, WPAFB OH 45433-6583

AFIT/GNE/ENP/92M

IC&C Idaho, Inc.

P.O. Box 1625

Idaho Falls, ID 83415

ATTN: Garland L. Stanley

Approved for public release; distribution unlimited

Nuclear thermal propulsion offers significant improvements in rocket engine specific impulse over rockets employing chemical propulsion. The computer code ATHENA (Advanced Thermal Hydraulic Energy Network Analyzer) was used in a parametric analysis of a fuelpipe. The fuelpipe is an annular particle bed fuel element of the reactor with radially inward flow of hydrogen through it. The outlet temperature of the hydrogen is parametrically related to key effects, including the effect of reactor power at two different pressure drops, the effect of the power coupling factor of the Annular Core Research Reactor, and the effect of hydrogen flow. Results show that the outlet temperature is linearly related to the reactor power and nonlinearly to the change in pressure drop. The linear relationship at higher temperatures is probably not valid due to dissociation of hydrogen. Once thermal properties of hydrogen become available, the ATHENA model for this study could easily be modified to test this conjecture.

Nuclear Propulsion, Nuclear Reactors, ATHENA,  
Propulsion Systems, Computerized Simulation

72

Unclassified

Unclassified

Unclassified

UL